AVERAGE CHANNEL CAPACITY OF FREE-SPACE OPTICAL MIMO SYSTEMS OVER ATMOSPHERIC TURBULENCE CHANNELS

Ha Duyen Trung[1], Duong Huu Ai [1] and Anh Tuan Pham [2]

[1] School of Electronics and Telecommunications, Hanoi University of Science and Technology, Hanoi, Vietnam, e-mail: trung.haduyen@hust.edu.vn

[2] Computer Communication Laboratory, The University of Aizu, Fukushima, Japan

Received Date: November 26, 2014

Abstract

In this paper, we theoretically analyze the performance of multiple-input multiple-output (MIMO) free-space optical (FSO) systems. The MIMO/FSO average channel capacity (ACC), which is expressed in terms of average spectral efficiency (ASE) is derived taking into account the atmospheric turbulence effects on the MIMO/FSO channel. They are modeled by log-normal and the gamma-gamma distributions for the cases of weak-to-strong turbulence conditions. We quantitatively discuss the influence of turbulence strength, link distance, and different MIMO configurations on the system ASE. Numerical and computer simulation results are presented in order to verify the validity of the mathematical analysis.

Keywords: Channel capacity, Free-space optical communications, MIMO

Introduction

Free-space optical (FSO) communications, a cost-effective, license-free, high security and high bandwidth access technique, has received considerable attention recently for a variety of applications [1]. One of major degradations to the performance of FSO communications is the influence of atmospheric turbulence caused by variations in the refractive index due to inhomogeneity in temperature, pressure fluctuations in the air along the propagation path of the laser beam [2].

Recent studies have revealed that, similar to wireless communications, the effect of turbulence on FSO links can be significantly reduced by employing a multiple-input multiple-output (MIMO) with multiple lasers at the transmitter and multiple photodetectors at the receiver. The first use of advantage of spatial diversity in FSO systems has been proposed in [3]. In [4] and [5] Lee *et al.* have derived the outage probability of FSO MIMO systems over log-normal turbulence channels assuming Gaussian noise statistics. In [6]-[9], D. Takase and T. Ohtsuki have proposed optical wireless multiple-input multiple-output (OMIMO) communications to achieve high speed transmission with a compact transmitter and receiver. The signal-to-interference-plus-noise ratio (SINR) and the bit error rate (BER) of the proposed OMIMO have also analysed with a linear array assignment of optical transmit and receive antennas, and employing subcarrier multiplexing (SCM) for each optical transmit antenna.

In [10] and [11] Wilson *et al.* have formulated and analyzed symbol error probability (SEP) and bit error probability (BEP) of FSO MIMO transmissions assuming pulse position modulation (PPM) and *Q*-ary PPM in both log-normal and Rayleigh fading channels. In all of these studies however, FSO systems using either OOK or PPM signaling are considered thanks to its simplicity and low cost. Whereas, because of the presence of atmospheric turbulence, OOK modulation requires to select adaptive thresholds appropriately to achieve

its optimal performance and PPM modulation has poor bandwidth efficiency. In order to overcome the limitations of OOK and PPM, FSO systems using sub-carrier (SC) intensity modulation schemes, such as sub-carrier phase shift keying (SC-PSK) and sub-carrier quadrature amplitude modulation (SC-QAM), have been proposed. The use of the SC intensity modulation scheme also allows the combination of several radio frequency SC streams into an intensity modulated laser signal, which results in the higher system throughput and flexibility in signal multiplexing. The performance of FSO systems using SC-PSK has been extensively investigated [12]-[15]. Regarding the SC-QAM systems, the average SEP of the FSO SISO systems using SC-QAM over atmospheric turbulence channel can be found in [16]. Recently, in [17] Hassan *et al.* presented the ASER for sub-carrier intensity modulated wireless optical communications using SC-QAM and series expansion of the modified Bessel function from [18], in [19] Trung presented the ASER of MIMO/FSO system using SC-QAM signals. Most recently, In [20] present the BER performance of single-input multiple-output (SIMO), multiple-input single-output (MISO) and multiple-input multiple-output (MIMO) FSO systems over this new channel model described by the Double Generalized Gamma distribution which is a new generic statistical model covering all turbulence conditions.

In addition to ASER performance, average capacity performance for MIMO/FSO systems is recently reported in [21]-[23]. In [21] Deng *et al.* presented analytic expressions and statistical models of the scintillation index and average capacity for multiple partial coherent beams propagating through strong turbulence MIMO FSO links. In [22] Sharma *et al.* evaluated the capacity of MIMO-OFDM/FSO with intersymbol interference (ISI) under strong atmospheric turbulence conditions. In [23] Duy derived closed-form expressions for the average capacity of MIMO FSO systems over Gamma-Gamma fading channel model using both equal gain combining and maximal ratio combining diversity techniques. However, to the best of our knowledge, the performance on average channel capacity of MIMO/FSO systems for both weak and strong atmospheric turbulence channels has not been clarified.

In this work, we therefore present a comprehensive study on the performance of FSO employing MIMO configurations in order to improve systems' capacity performance over atmospheric turbulence channels. In particular, we theoretically derive and discuss the MIMO/FSO average channel capacity (ACC), which is expressed in terms of average spectral efficiency (ASE), under the impact of various channel conditions, system parameters and configurations. The numerical results that generated by analytical formulas accurately approximate computer simulation results.

The remainder of the paper is organized as follows. In Section 2 the system descriptions are described in detail. In Section 3 atmospheric turbulence models are presented. In Section 4 channel capacity of MIMO/FSO links is derived for weak and strong turbulence channels. In the Section 5 the numerical and simulation results are presented, analyzing the influence of turbulence strength, link distance and various MIMO configurations on the systems' ASE. The paper concludes with a summary given in the end.

System Descriptions

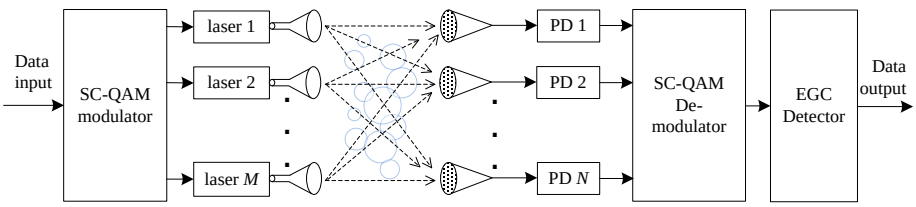

Figure 1. Block diagram of $M \times N$ FSO MIMO system using SC-QAM signals over atmospheric turbulence channel

We consider a general $M\times N$ FSO MIMO system using SC-QAM signals with M transmitting lasers pointing toward an N-aperture receiver as depicted in Figure 1. Data transmission employing the same SC-QAM signal is transmitted with perfect synch-ronization by each of the M transmit telescopes through a turbulence channel toward N photodetectors (PDs) with the light beamwidths of each telescope assume to be wide enough to illuminate the entire receiver array. The transmitter's telescope array is assumed to produce the same total optical power irrespective of M to enforce a fair comparison with the single transmitter case. The distance between the individual transmit telescope and receive telescope is assumed to be sufficient so that spatial correlation is negligible.

The MIMO channel is modeled and can be denoted by an $M\times N$ matrix of the turbulence channel $\mathbf{X}=\left[X_{mn}(t)\right]\Big|_{m,n=1}^{M,N}$. The electrical signal at the output of the PD corresponding to the nth receive aperture output can be expressed as follows

$$r_e^{(n)}(t)=\Re P_s\kappa e(t)\sum_{m=1}^{M}X_{mn}(t)+\upsilon^n(t),n=1,2...,N, \tag{1}$$

where $\Re$ is PD's responsivity, P_s denotes the average transmitted optical power per symbol, κ is the modulation index, *e(t)* represents the electrical QAM signal, $X_{mn}(t)$ denotes the stationary random process for the turbulence channel between the mth laser to the nth PD. The X_{mn}'s are uncorrelated with independent and identically distributed (i.i.d.) random variables (RVs). $\upsilon^n(t)$ is the AWGN with zero mean and variance $N_0^{(n)}$. Assuming the equal gain combining (EGC) detector is employed at the receiver to estimate the transmitted signal. Such that Equation (1) is valid with $\upsilon(t)=\sum_{n=1}^{N}\upsilon^{(n)}(t)$, and the combined electrical intensity at the receiver output can be expressed as

$$y_e(t)=\sum_{n=1}^{N}r^{(n)}(t)=\Re P_s\kappa e(t)\sum_{n=1}^{N}\sum_{m=1}^{M}X_{mn}+\upsilon(t). \tag{2}$$

Under the assumption of perfect channel estimation at the receiver side, the conditional input SNR, γ, at the PD can be written as a finite sum of sub-channel SNRs as

$$\gamma=\left(\sum_{m=1}^{M}\sum_{n=1}^{N}\sqrt{\gamma_{mn}}\right)^2=\left(\sum_{m=1}^{M}\sum_{n=1}^{N}\sqrt{\overline{\gamma}_{mn}}X_{mn}\right)^2, \tag{3}$$

where γ_{mn} are RVs defined as the instantaneous electrical SNR at the output of the nth PD caused by signal from the mth laser. γ_{mn} are given in the following

$$\gamma_{mn}=\left(\frac{1}{MN}X_{mn}\Re P_s\kappa\right)^2\Big/N_0=\overline{\gamma}_{mn}X_{mn}^2, \tag{4}$$

in which, we denote N_0 is the total noise variance and $\overline{\gamma}_{mn}$ is the average SNR contributed by the sub-channel between the m^{th} laser and the n^{th} PD. $\overline{\gamma}_{mn}$ is given by

$$\overline{\gamma}_{mn}=\left(\frac{1}{MN}\Re P_s\kappa\right)^2/N_0. \tag{5}$$

Atmospheric Turbulence Models

There are several statistical models that can be used to describe irradiance fluctuation. For weak atmospheric turbulence condition, the turbulence included fading is assumed to be a random process that follows that log-normal distribution [12], whereas for strong turbulence conditions, a gamma-gamma distribution is used [24].

The Log-Normal Turbulence Model

In log-normal fading channel, the probability density function (pdf) for an normalized irradiance with log-normal RV, $X_{mn} \geq 0$, is described as [12]

$$f_{X_{mn}}(x) = \frac{1}{x\sigma_s\sqrt{2\pi}} \exp\left(-\frac{(\ln(x) + \frac{\sigma_s^2}{2})^2}{2\sigma_s^2} \right), \tag{6}$$

where $\sigma_s^2 = \exp(\psi_1 + \psi_2) - 1$ with ψ_1 and ψ_2 are respectively given by

$$\begin{aligned} \psi_1 &= \frac{0.49\sigma_2^2}{\left(1 + 0.18d^2 + 0.56\sigma_2^{12/5}\right)^{7/6}} \\ \psi_2 &= \frac{0.51\sigma_2^2}{\left(1 + 0.9d^2 + 0.62\sigma_2^{12/5}\right)^{5/6}}. \end{aligned} \tag{7}$$

In Equation (7), $d = \sqrt{kD^2/4L}$, where $k = 2\pi/\lambda$ is the optical wave number, L is the link distance in meters, λ is the optical wavelength, and D is the receiver aperture diameter of the PD. The parameter σ_2^2 is the Rytov variance and in this case, is expressed by [24]

$$\sigma_2^2 = 1.23 C_n^2 k^{7/6} L^{11/6}, \tag{8}$$

where C_n^2 stands for the strength of the atmospheric turbulence, which is the altitude-dependent and varying from 10^{-17} to $10^{-13}\text{m}^{-2/3}$ according to the turbulence conditions.

The Gamma-Gamma Turbulence Model

The pdf of a normalized gamma-gamma RV, $X_{mn} \geq 0$, arises from the product of two independent gamma distributed RVs and given as [24]

$$f_{X_{mn}}(x) = \frac{2(\alpha\beta)^{\frac{\alpha+\beta}{2}}}{\Gamma(\alpha)\Gamma(\beta)} x^{\frac{\alpha+\beta}{2}-1} K_{\alpha-\beta}\left(2\sqrt{\alpha\beta x}\right), \tag{9}$$

where $\Gamma(\alpha)$ is the Gamma function and $K_{\alpha-\beta}(\cdot)$ is the modified Bessel function of the second kind of order $(\alpha - \beta)$, while the parameters α and β are directly related to atmospheric conditions through the following expressions:

$$\alpha = \left[\exp(\psi_1) - 1\right]^{-1}, \tag{10}$$

$$\beta = \left[\exp(\psi_2) - 1\right]^{-1}. \tag{11}$$

Average Channel Capacity

In this section, we analytically derive the average channel capacity (ACC) for the $M\times N$ MIMO/FSO link in the presence of atmospheric turbulences. This is a crucial metric for evaluating the optical link performance. The ACC can also be expressed in terms of average spectral efficiency (ASE) in bits/s/Hz if the frequency response of the channel is known. We assume that the optical channel is memoryless, stationary, ergodic with i.i.d. turbulence statistics and perfect channel state information (CSI) is available at both the transmitting lasers and the aperture receivers, the system ASE can be defined as

$$\frac{\overline{C}}{B}=\int_{\Gamma}\log_2\left(1+\gamma\right)\times f_{\Gamma}(\Gamma)d\Gamma,\quad \text{(bit/s/Hz)} \tag{12}$$

where B is the channel' bandwidth and is the total channel SNR and $\Gamma=\left\{\gamma_{nm},n=1,...,N,m=1,...,M\right\}$ is the matrix of the MIMO atmospheric turbulence channels. The joint p.d.f $f_{\Gamma}(\Gamma)$ can be reduced to a product of the firt-order p.d.f of each element γ_{nm}. The pdfs of Γ are respectively described in log-normal and gamma-gamma distributions as follows

$$f(\gamma_{mn})=\frac{1}{2\gamma_{mn}\sigma_s\sqrt{2\pi}}\exp\left(-\frac{(\ln(\frac{\gamma_{mn}}{\overline{\gamma}})+\sigma_s^2)^2}{8\sigma_s^2}\right), \tag{13}$$

$$f(\gamma_{mn})=\frac{(\alpha\beta)^{\frac{\alpha+\beta}{2}}}{\Gamma(\alpha)\Gamma(\beta)}\frac{\gamma_{mn}^{\frac{\alpha+\beta}{4}-1}}{\overline{\gamma}^{\frac{\alpha+\beta}{4}}}K_{\alpha-\beta}\left(2\sqrt{\alpha\beta\sqrt{\frac{\gamma_{mn}}{\overline{\gamma}}}}\right). \tag{14}$$

Capacity Of Log-Normal MIMO/FSO Channels

Using (12) and (13), the ASE of a log-normal MIMO/FSO channel capacity can be expressed as

$$\frac{\overline{C}}{B}=\frac{1}{2\sigma_s\sqrt{2\pi}\ln(2)}\int_{\Gamma}\frac{\ln\left(1+\gamma_{mn}\right)}{\gamma_{mn}}\times\exp\left(-\frac{\left(\ln\left(\frac{\gamma_{mn}}{\overline{\gamma}_{mn}}\right)+\sigma_s^2\right)^2}{8\sigma_s^2}\right)d\gamma_{mn}. \tag{15}$$

Using the equality $\ln(1+x)=\sum_{k=1}^{+\infty}(-1)^{k+1}x^k/k,\ \left(0\le k\le 1\right)$, and the scaled complementary error function $\text{erfc}(x)=e^{x^2}\,\text{erfc}(x)$, the integral can be transformed to the summation as follows

$$\frac{\overline{C}}{B}=C_0\left(\sum_{k=1}^{\infty}\frac{(-1)^{k+1}}{k}\left[\operatorname{erfc}\left(\sqrt{2}\sigma_s k+\frac{\Gamma_{mn}}{2\sqrt{2}\sigma_s}\right)\right.\right.$$
$$\left.+\operatorname{erfc}\left(\sqrt{2}\sigma_s k-\frac{\Gamma_{mn}}{2\sqrt{2}\sigma_s}\right)\right]+\frac{4\sigma_s}{\sqrt{2\pi}}+\Gamma_{mn} \quad (16)$$
$$\left.\times\exp\left(\frac{\Gamma_{mn}^2}{8\sigma_s^2}\right)\operatorname{erfc}\left(-\frac{\Gamma_{mn}}{2\sqrt{2}\sigma_s}\right)\right),$$

In Equation (16), $\Gamma_{mn}=\ln(\overline{\gamma}_{mn})-\sigma_s^2$ with $\overline{\gamma}_{mn}$ is the instantaneous received SNR output of EGC detector, and $C_0=\exp(-\Gamma^2/8\sigma_s^2)/2\ln 2$.

Capacity Of Gamma-Gamma MIMO/FSO Channels

Substituting (14) into (12), the average capacity of a gamma-gamma MIMO/FSO channel can be given by

$$\frac{\overline{C}}{B}=\frac{\left(\frac{\alpha\beta}{\sqrt{\overline{\gamma}_{mn}}}\right)^{\frac{\alpha+\beta}{2}}}{\Gamma(\alpha)\Gamma(\beta)\ln(2)}\int_{\Gamma}\ln(1+\gamma_{mn})$$
$$\times\gamma_{mn}^{\frac{\alpha+\beta}{4}-1}K_{\alpha-\beta}\left(2\sqrt{\alpha\beta\sqrt{\frac{\gamma_{mn}}{\overline{\gamma}_{mn}}}}\right)d\gamma_{mn}. \quad (17)$$

Using the Meijer *G*-function, $G_{mn}^{pq}[\cdot]$, to express the logarithmic term of $\ln(1+x)=G_{2,2}^{1,2}\left[x\middle|_{1,0}^{1,1}\right]$, and $K_{\upsilon}=\frac{1}{2}G_{0,2}^{2,0}\left[\frac{x^2}{4}\middle|_{\frac{\upsilon}{2},-\frac{\upsilon}{2}}^{-,\ -}\right]$, the ASE can be given by

$$\frac{\overline{C}}{B}=\frac{\left(\frac{\alpha\beta}{\sqrt{\overline{\gamma}_{mn}}}\right)^{\frac{\alpha+\beta}{2}}}{4\pi\Gamma(\alpha)\Gamma(\beta)\ln(2)}G_{2,6}^{6,1}\left[\frac{(\alpha\beta)^2}{16\overline{\gamma}_{mn}}\middle|_{\frac{p}{4},\frac{p+2}{4},-\frac{p}{4},-\frac{c}{4},-\frac{c}{4}}^{-\frac{c}{4},-\frac{c}{4}+1}\right], \quad (18)$$

where $c=\alpha+\beta$ and $p=\alpha-\beta$.

Numerical and Simulation Results

Using derived expressions of (16) and (18), we evaluate the ASE of MIMO/FSO channels as a function of the average electrical SNR at the receiver, $\overline{\gamma}$. We use (16) for the case of weak turbulence with log-normal distribution model, while (18) is used for strong case with the gamma-gamma distribution. We use the system parameters and three different values of turbulence strength and link distance, C_n^2, *L*. Here, SISO/FSO channel is also included in the numerical results as a benchmark. Expressions derived in (16) and (18) both give approximately the same results and are identical to the results obtained by computer simulations. However, the accuracy of the cases of weak turbulence is higher than that of the case of strong turbulence. The reason of this is results obtained from Equation (16) are more accuracy than results obtained from Equation (18).

Figures 2-4 illustrate the ASE of different MIMO/FSO channels (i.e. 2×2 and 4×4 MIMO/ FSO channels) with respect to $\bar{\gamma}$, for three values of the turbulence strength C_n^2 (i.e., $C_n^2 = 10^{-15}\ \mathrm{m}^{-2/3}$, $C_n^2 = 9\times10^{-15}\ \mathrm{m}^{-2/3}$, and $C_n^2 = 3\times10^{-14}\ \mathrm{m}^{-2/3}$, for weak, moderate and strong turbulence conditions, respectively), and with three different link distances (L = 1000, 3000 m, and 6000 m). It can be also seen that the ASE strongly depends on the atmospheric turbulence strength, and as the link distance gets longer, the influence of atmospheric turbulence becomes stronger. Obviously, the ASE under the weak turbulence conditions is higher than in the cases of moderate and strong turbulence, especially with longer link distance L. The reason of this is that as optical link distance gets longer, the signal propagates in the atmospheric with longer distances; the influence of the turbulence therefore becomes stronger. On the other hand, as expected, the ASE could be improved by approximately 2 (b/s/Hz) when the system is upgraded from SISO/FSO to 2×2 MIMO/FSO or from 2×2 MIMO/FSO to 4×4 MIMO/FSO.

Figure 5 depicts the ASE of 2 × 2 MIMO/FSO channel with respect to, using subcarrier-multilevel QAM (i.e. 16 SC-QAM, 32 rectangular SC-QAM, 32 square SC-QAM, and 64 SC-QAM) for weak atmospheric turbulence strengths, $C_n^2 = 10^{-15}\ \mathrm{m}^{-2/3}$ under free-space link distance L = 3000 m. ASE of SISO/FSO channel is also plotted in the Figure 5 as a benchmark. It is clearly shown that the ASE performance is improved significantly with the increase of number of lasers and receivers. More specifically, when the modulation level changes from 16 to 32 and 64 SC-QAM, a significant channel capacity increase is observed for the same SNR. In addition, as expected, ASE increases as number of lasers M and receiver N increase from SISO to 2×2 MIMO, it results in an average gain of approximately 2 bps/Hz at the same SNR.

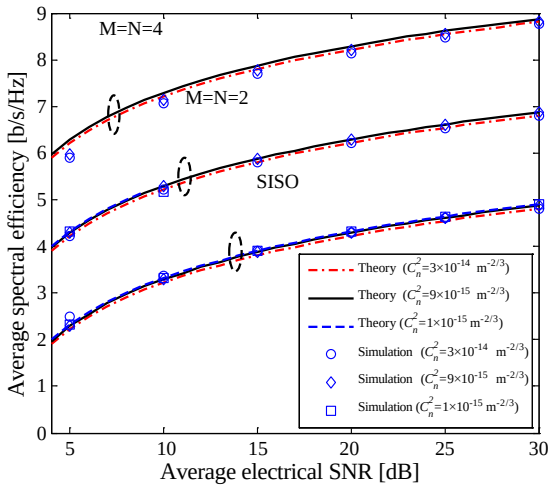

Figure 2. ASE, $\bar{C}/B$, versus the average electrical SNR, $\bar{\gamma}$, of various MIMO/FSO channels for weak to strong atmospheric turbulence strengths, C_n^2 under link distance L=1000 m.

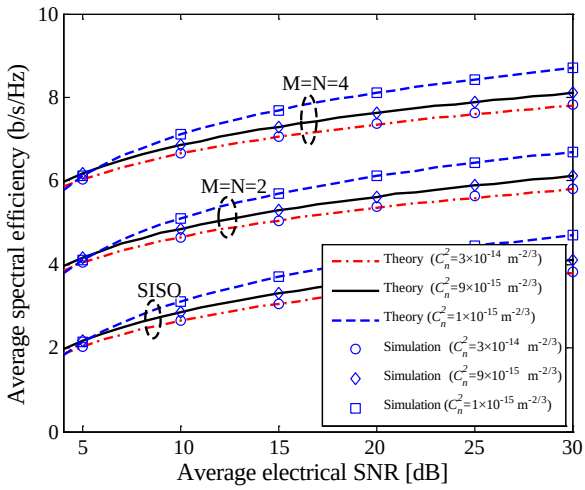

Figure 3. ASE, $\bar{C}/B$, versus the average electrical SNR, $\bar{\gamma}$, of different MIMO/FSO channels for weak to strong atmospheric turbulence strengths, C_n^2 under link distance L=3000 m.

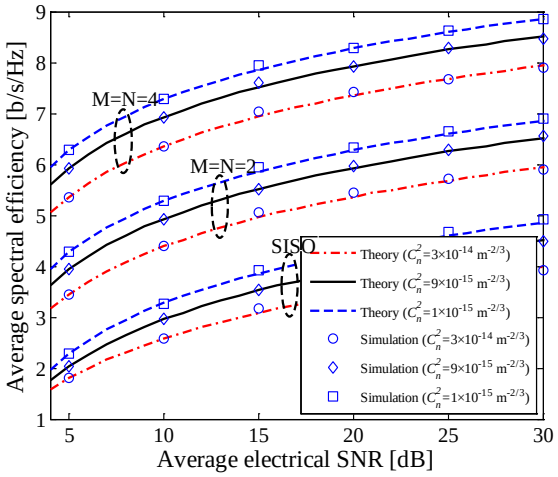

Figure 4. ASE, $\bar{C}/B$, versus the average electrical SNR, $\bar{\gamma}$, of different MIMO/FSO channels for weak to strong atmospheric turbulence strengths, C_n^2 under link distance L=6000 m.

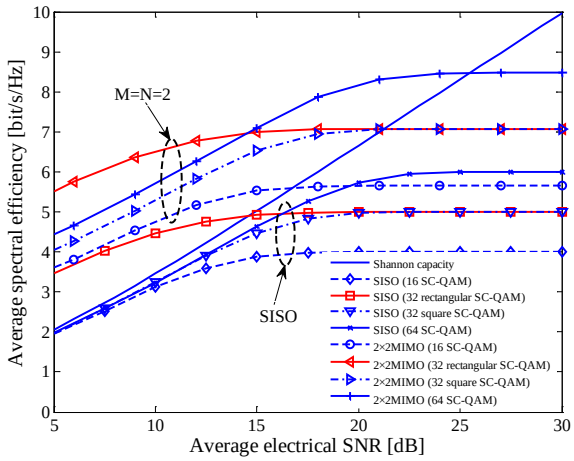

Figure 5. ASE, $\bar{C}/B$, versus the average electrical SNR, $\bar{\gamma}$, ASE versus average SNR of different MIMO/FSO channels using different multilevel QAM modulation for weak atmospheric turbulence strength under the link distance L=3000m.

Conclusions

We have presented the performance analysis on the average channel capacity of MIMO/FSO systems using SC-QAM signals over atmospheric turbulence channels. The log-normal and gamma-gamma distribution models were used to describe the fluctuation of the optical propagating over atmospheric turbulence channels. We analytically derived the system ASE considering different link conditions and MIMO configurations. The numerical results showed that, with the similar link distance and turbulence strength, regardless the link distance and turbulence condition, the ASE of the FSO link could be improved by approximately 2 (b/s/Hz) when the system is upgraded from SISO/FSO to 2×2 MIMO/FSO or from 2×2 MIMO/ FSO to 4×4 MIMO/FSO. The derived results were compared with the computer simulations in order to verify the correctness of the performance analysis.

References

[1] D. Kedar, and S. Arnon, "Urban optical wireless communication networks: The main challenges and possible solutions," *IEEE Communications Magazine*, Vol. 42, No. 5, pp. 2-7, 2004.

[2] X. Zhu, and J.M. Kahn, "Free-space optical communication through atmospheric turbulence channels," *IEEE Transactions on Communications*, Vol. 50, No. 8, pp. 1293–1300, 2002.

[3] M.M. Ibrahim, and A.M. Ibrahim, "Performance analysis of optical receivers with space diversity reception," In: *IEEE Proceedings-Communications*, Vol. 143, No. 6, pp. 369-372, 1996.

[4] E. Lee, and V. Chan, "Part 1: Optical communication over the clear turbulence atmospheric channel using diversity," *IEEE Transactions on Communications*, Vol. 22, No. 9, pp. 1896-1960, 2004.

[5] E.J. Shin, and V.W.S. Chan, "Optical communication over the turbulent atmospheric channel using spatial diversity," In: *IEEE Global Telecommunications Conference (GLOBECOM)*, pp. 2055-2060, 2002.
[6] D. Takase, and T. Ohtsuki, "Optical wireless MIMO communications (OMIMO)," In: *IEEE Global Telecommunications Conference (GLOBECOM'2004)*, pp. 928–932, 2004.
[7] D. Takase, and T. Ohtsuki, "Performance analysis of optical wireless MIMO with optical beat interference," In: *IEEE International Conference on Communications (ICC2005)*, pp. 954–958, 2005.
[8] D. Takase, and T. Ohtsuki, "Spatial multiplexing in optical wireless MIMO communications over indoor environment," *IEICE Transactions on Communications*, Vol. E89-B, No. 4, pp. 1364–1371, 2006.
[9] D. Takase, and T. Ohtsuki, "Optical wireless MIMO (OMIMO) with backward spatial filter (BSF) in diffuse channels," In: *IEEE International Conference on Communications (ICC2007)*, pp. 2462–2467, 2007.
[10] S.G. Wilson, M. Brandt-Pearce, Q. Cao, and J.H. Leveque, "Free-space optical MIMO transmission with *Q*-ary PPM," *IEEE Transactions on Communications*, Vol. 53, No. 8, pp. 1402-1412, 2005.
[11] S.G. Wilson, M. Brandt-Pearce, Q. Cao, and J.H. Leveque, "Optical repetition MIMO transmission with multiple PPM," *IEEE Journal on Selected Areas in Communications*, Vol. 23, No. 9, pp. 1901-1910, 2005.
[12] J. Li, J.Q. Liu, and D.P. Taylor, "Optical communication using subcarrier PSK intensity modulation through atmospheric turbulence channels," *IEEE Transactions on Communications*, Vol. 55, No. 8, pp. 1598-1606, 2007.
[13] W.O. Popoola, and Z. Ghassemlooy, "BPSK subcarrier intensity modulated free-space optical communications in atmospheric turbulence," *Journal of Lightwave Technology*, Vol. 27, No. 8, pp. 967-973, 2009.
[14] A. Pham, T. Thang, S. Guo, and Z. Cheng, "Performance bounds for turbo-coded sc-psk/fso communications overstrong turbulence channels," In: *IEEE International Conference on Advanced Technologies for Communications (ATC'11)*, pp. 161-164, 2011.
[15] X. Song, M. Niu, and J. Cheng, "Error rate of subcarrier intensity modulations for wireless optical communications," *IEEE Communications Letters*, Vol. 16, pp. 540-543, 2012.
[16] K.P. Peppas, and C.K. Datsikas, "Average symbol error probability of general-order rectangular quadrature amplitude modulation of optical wireless communication systems over atmospheric turbulence channels," *Journal of Optical Communications and Networking*, Vol. 1, No. 2, pp. 102-110, 2010.
[17] M.D.Z. Hassan, X. Song, and J. Cheng, "Subcarrier intensity modulated wireless optical communications with rectangular QAM," *Journal of Optical Communications and Networking*, Vol. 4, No. 6, pp. 522-532, 2012.
[18] E. Bayaki, R. Schober, and R.K. Mallik, "Performance analysis of MIMO free-space optical systems in gamma-gamma fading," *IEEE Transactions on Communications*, Vol. 57, No. 11, pp. 3415-3424, 2009.
[19] H.D. Trung, "Aser analysis of free-space optical MIMO systems using sub-carrier QAM in atmospheric turbulence channels," *Journal of Science and Technology*, No. 95, pp. 116-123, 2013.

[20] M. Aminikashani, M.U, and M. Kavehrad, "On the Performance of MIMO FSO Communications over Double Generalized Gamma Fading Channels," In: *Proceedings of 2015 IEEE International Conference on Communications (ICC)*, pp. 5144-5149, 2015.
[21] P. Deng, M. Kavehrad, Z. Liu, Z. Zhou, and X. Yuan, "Capacity of MIMO free space optical communications using multiple partially coherent beams propagation through non-Kolmogorov strong turbulence," *Optics Express*, Vol. 21, No. 13, pp. 15213-15229, 2013.
[22] M. Sharma, D. Chadha, and V. Chandra, "Evaluation of the capacity of MIMO-OFDM free space optical communication system in strong turbulent atmosphere," In: *Proceedings of the 2013 International Conference on Wireless Networks*, 2013.
[23] D.A. Luong and T.A. Pham, "Average capacity of MIMO free-space optical gamma-gamma fading channel," In: *Proceedings of IEEE International Conference on Communications (ICC 2014)*, Sydney, pp. 3354-3358, 2014.
[24] A.K. Majumdar, "Free-space laser communication performance in the atmospheric channel," *Journal of Optical and Fiber Communications Reports*, Vol. 2, No. 4, pp. 345-396, 2005.